TROPICAL PACIFIC LONG WAVES FOR THE 1994-1998 EL NIÑO-LA NIÑA EVENT FROM AN ALTIMETRIC DATA ASSIMILATION EXPERIMENT

B. Dewitte[(1)], S. Illig[(2)], L. Parent[(3)], Y. duPenhoat[(1)], L. Gourdeau[(1)] and J. Verron[(3)]

[(1)] LEGOS/IRD, 14 av. Edoaurd Belin, Toulouse, France
[(2)] JPL/NASA, CA 91109, Pasadena, USA
[(3)] LEGI, BP53, 38041 Grenoble, France

ABSTRACT

A forced Ocean General Circulation Model simulation of the tropical Pacific in which combined TOPEX/POSEIDON and ERS altimetric data over January 1994-July 1999 are assimilated, is used to investigate equatorial wave characteristics during the intense 1997-1998 El Niño-La Niña event. The assimilation results in an increased contribution of the higher-order baroclinic modes in the eastern basin and a decreased contribution of the first baroclinic mode in the western Pacific for the zonal current variability. Kelvin and first meridional Rossby waves are then derived for the first two more energetic baroclinic modes. The Kelvin waves of both modes contribute constructively to the strong warming observed in 1997, with the first (second) baroclinic mode being more energetic than the (first) second baroclinic mode in the early (mature) stage of the warming. Kelvin waves of both modes reflects as first meridional Rossby waves at the eastern boundary (reflection efficiency of ~ 95%) and contribute to push back the warm pool westward. From January 1998, the reversal of the warming is apparently initiated by the second baroclinic mode contribution which controls the position of the 28°C isotherm at the surface. At the western boundary, reflection of Rossby waves takes place for both modes, but a ~50% reflection efficiency is derived at 165°E. This suggests that the delayed oscillator theory is not applicable for explaining the reversal from warm to cold conditions during the 1997-1998 El Niño-La Niña, while the zonal advective feedback was at work. This study suggests that it is necessary to take into account the vertical structure of the ocean when interpreting altimetric data, which can be done through assimilation experiment.

1. INTRODUCTION

From recent modelling and observational studies, there is increasing evidence that the vertical structure of the low frequency variability found in the tropical Pacific Ocean cannot reduce to a single mode, i.e. the first baroclinic mode [1, 2, 3]. Because the sea level anomaly is an integrated information of the stratification variability over the whole water column, the studies of the equatorial waves from the only information of the TOPEX/POSEIDON data for instance requires to assume that they are mostly representative of the first baroclinic mode only (namely that the equatorial pacific reduces to two layers, an active upper layer and the other below at rest). These studies brought some insights on the mechanisms at work during the 1997 El Niño event in particular. However they cannot avoid limitations due to the one-mode approximation, which includes the uncertainties in the estimate of the reflectivity of the meridional boundaries and the amplitude of the wave coefficients itself.

Assimilation experiments of altimetric data offer the opportunity to estimate the baroclinic mode contributions to sea level anomalies and study the equatorial wave characteristics according to the most energetic baroclinic modes and refine the interpretation of surface observations. Outputs from an assimilation of TOPEX/POSEIDON and ERS derived sea level anomalies in a primitive equation model [4] are here used to investigate the long equatorial wave's characteristics during the 1994-1998 period with a focus on the 1997-1998 El Niño event.

The impact of the assimilation of altimetric data on the vertical structure is first illustrated. In particular the assimilation results in a redistribution of energy on the baroclinic modes and consequently modifies the equatorial waves characteristics compared to the control run (no assimilation). The results of a meridional mode decomposition (Kelvin and Rossby waves) according the gravest baroclinic modes are then analysed. In the light of the existing ENSO theories, we provide new insights for explaining the processes at work during the reversal from El Niño to La Niña in 1998.

2. ASSIMILATION EXPERIMENT DESCRIPTION

2.1 The model

The OPA Ocean General Circulation Model [5] is used. The domain covers the tropical Pacific from 120°E to 75°W, 30°N to 30°S, with realistic coastline and bathymetry. The zonal resolution is 1°, and the

meridional resolution varies from 0.5° in the equatorial wave-guide to 2° at the northern and southern boundaries. There are 25 vertical levels with a 10 meter resolution at the surface down to 120 meters. The surface fluxes of momentum results from a combination of ERS1-2 scatterometer derived wind stresses and TAO derived stresses [6]. The other surface boundary conditions come from the NCEP/NCAR reanalysis. SST and SSS fields are relaxed towards observed SST [7] and climatological SSS.

2.2 The SEEK filter

The assimilation method used, named the SEEK filter, is sequential and based on the extended Kalman filter. It was introduced by [8] and validated by twin experiments in the tropical Pacific Ocean by [9]. With such an approach, as in similar approaches (e.g. [10]), the general idea is to reduce the enormous computing requirements by projecting the prediction error covariance matrix in a reduced space. The reduced space is defined through a convenient MEOF analysis of free model outputs. The SEEK filter is applied to the assimilation of the T/P+ERS data into the OPA model in the same way as it was by [11]. Gridded data are assimilated every 10 days. The assimilation experiment, hereafter referred as ASSIM, was performed over a 5-year period of the T/P mission from Jan. 1994 to Jul. 1999. The output used from the assimilation experiments is the forecast state, sampled every 10 days.

2. 3 The data

The gridded sea level anomaly data (SLA) were supplied by AVISO/altimetry. They were built by optimal interpolation of T/P and ERS data on a 1/4° x 1/4° grid every ten days. Subsurface temperature data base provided by the BMRC in Australia, and *in situ* temperature and current data from the TAO array were used to validate the assimilation results.

2. 3 Impact of the assimilation

Results from the assimilation of the 1994-1999 Topex/Poseidon sea level anomalies in the tropical Pacific OPA model are presented in [4]. Here, we focus on the impact of the assimilation on the vertical structure variability.

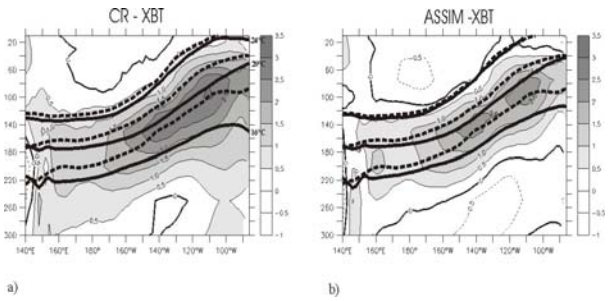

Figure 1: Equatorial mean temperature difference between *in situ* temperature data and the simulation without/with assimilation (a, b respectively) . Unit is °C and shading is for values larger than 0.5°C. The mean isotherms 16°C, 20°C and 24°C are represented in plain line for the simulation and in dashed line for the observations.

Fig. 1 illustrates that the mean thermocline depth is better simulated in the assimilation experiment with in particular a more realistic representation of the temperature vertical gradient.

A decomposition in vertical modes of the model variables is sought along the equator for both simulations (with and without assimilation). Only the first two baroclinic modes, the most energetic modes, are discussed here. Zonal currents {*u(x,y,z,t)*} and pressure {*p(x,y,z,t)*} anomalies are estimated relative to the climatological seasonal cycle of the 1994-1996 simulation (3 years). These fields are then projected on the estimated vertical structure functions *Fn(x,z)*.

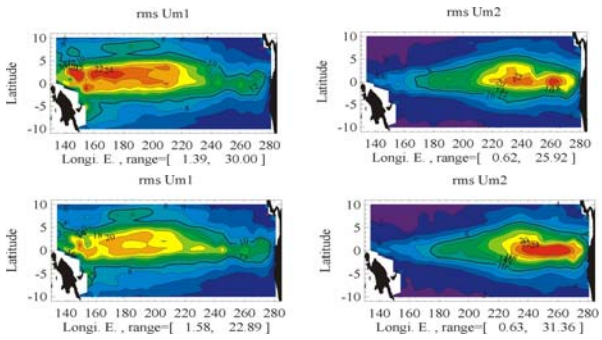

Figure 2: Contribution of the first (left) and second (right) baroclinic modes to the surface currents variability for the model without (top) and with (bottom) assimilation. Units are cm s^{-1} and contour intervals are 2 cm s^{-1}.

The assimilation results in a redistribution of the energy of the baroclinic modes: Mode 1 is less energetic in the western Pacific for the simulation with assimilation whereas Mode 2 is more energetic in the eastern Pacific for the simulation with assimilation. This impacts the equatorial waves characteristics.

3. LONG EQUATORIAL WAVES SEQUENCE DURING THE 1997-98 EL NIÑO-LA NIÑA

The 1997-1998 El Niño event caught the community by surprise not only by its intensity (SST anomalies reaching 6°C, cf. Fig. 3) but although by the rapidity of the shift to neutral to La Niña conditions. These characteristics can be interpreted in the light of

the results of the vertical mode decomposition of the assimilation run.

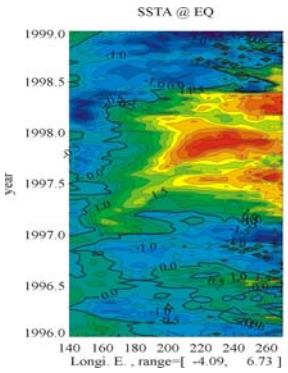

Figure 3: Longitude-time section of the simulated sea surface temperature anomalies in °C for the January 1996-January 1999 period along the equator.

In this section, we study the equatorial wave characteristics according to the first two more energetic baroclinc modes and their role on the termination of the 1997-1998 El Niño. For deriving the coefficient for the meridional modes, both the sea level and zonal current anomaly baroclinic contributions are projected onto the complete basis of the long-wavelength meridional modes. These are computed from the zonally varying phase speed obtained from the former vertical mode decomposition. The projection is performed between 10°S and 10°N. It was checked that the Kelvin and first-meridional Rossby mode contribution explained at least 80% of the variance in the 5°S-5°N band so that emphasis will be made on these two meridional modes.

The results of the decomposition are presented in Fig. 4 and Fig. 5 for the sea level anomalies.

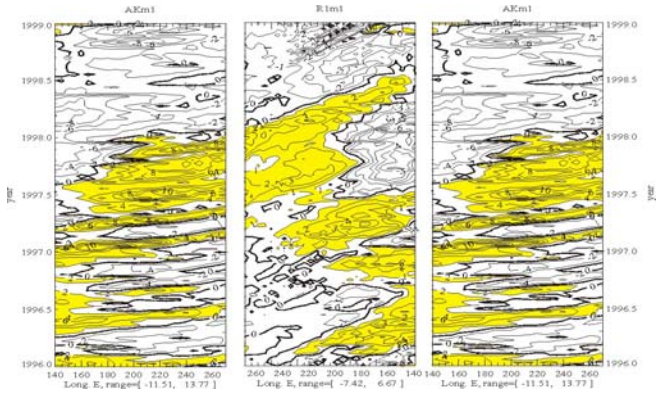

Figure 4: Longitude-time section of the (a) Kelvin (AK) and (b) first meridional Rossby mode (R1) contributions to sea level anomalies along the equator from January 1996 through January 1999 for the first baroclinic modes of the assimilation experiment. R1 is displayed in reverse from 270°E to 140°E and (c) AK is repeated to visualize wave reflections at boundaries. Contour intervals are 2 cm for AK and 1 cm for R1. The yellow shading is for anomalies larger than 2 cm (1 cm) for AK (R1). Note that linear theory predicts that, in the absence of modal dispersion, local wind-forcing and dissipation, the ratio of R1 (AK) versus AK (R1) should be ~1.22 (~0.44) near the eastern (western) boundary.

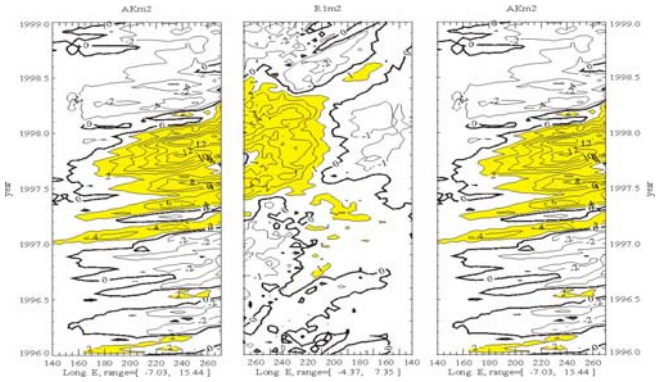

Figure 5: Same as fig. 4 but for the second baroclinic mode.

In December 1996, a westerly wind anomaly event near the western boundary forces a first and second baroclinic mode downwelling Kelvin waves (Figs. 4a and 5a). Their arrival at the NINO3 region corresponds to the end of cool conditions (Fig.3). Later in March 1997, strong westerly wind anomalies force another couple of first and second baroclinic mode downwelling Kelvin waves which amplify the warming in the eastern Pacific. Note that the ratio of the Kelvin wave amplitude between the first and second baroclinic modes is 50% weaker for the March 1997 wind event than for the December 1996 wind event, suggesting a change in the meridional scale and location of the wind events. Note also that, whereas the first baroclinic mode Kelvin wave generally undergoes a decrease in amplitude as it propagates eastward, the second baroclinic mode Kelvin wave amplitude increases from about 140°W. These two waves eventually reflect at the eastern boundary at slightly different times because of differences in propagation speed.

From mid-1997 onward, westerly wind anomalies develop near the date line in response to warmer SSTA in the eastern Pacific. In June–July 1997, wind anomalies around the dateline force strong downwelling Kelvin waves which induce strong eastward surface currents. At the same time, easterly wind anomalies develop in the eastern Pacific. They act against the positive SLA induced by the first-meridional Rossby waves, resulting from the reflection of the downwelling Kelvin waves. On the other hand, these easterlies force anomalous westward currents (i.e., with the same sign than the ones induced by the same Rossby wave contribution). It is at this time that the reversal toward cooler conditions is initiated, according to the Picaut et al. [11] mechanism which attributes to the

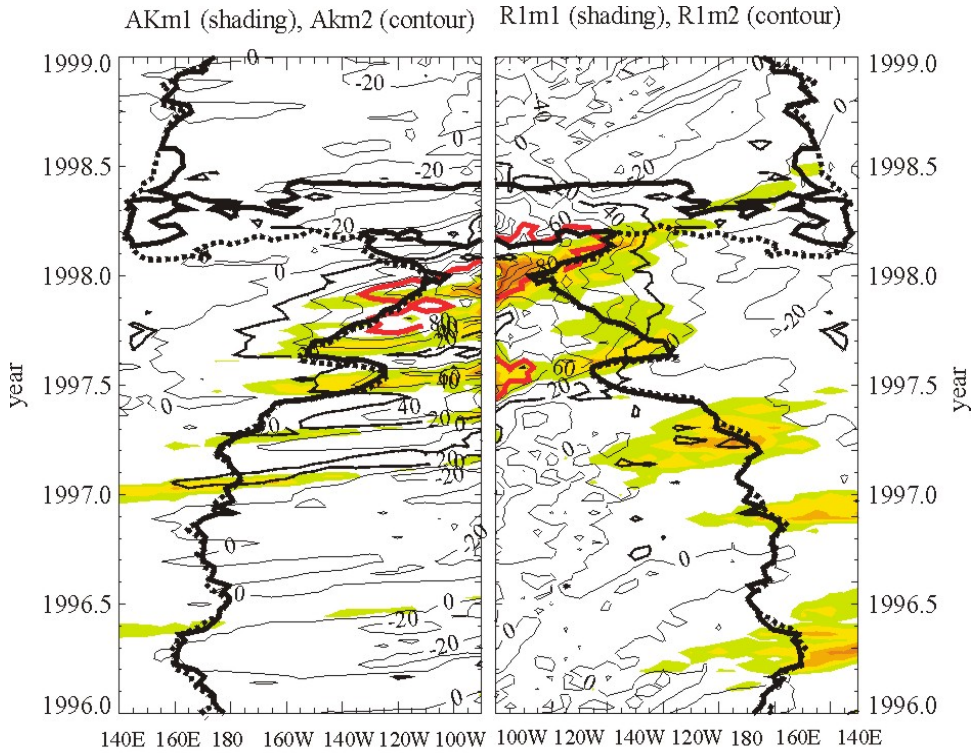

Figure 6: Longitude-time section of the (a) Kelvin and (b) first-meridional Rossby (displayed in reverse from 270°E to 140°E) mode contributions to zonal current anomalies along the equator from January 1996 through January 1999 for the first and second baroclinic modes. The shading (yellow scale) is for the first baroclinic mode Kelvin (first-meridional Rossby) wave amplitude whereas the contouring is for the second baroclinic mode Kelvin (first-meridional Rossby) wave amplitude. Contour intervals are 20 cm s^{-1}. The iso-line 80 cm s^{-1} is thicker and in red. The thick black dashed (dotted) line corresponds to the 28°C isotherm at 5 m (45 m). For the first baroclinic mode, only positive values are plotted.

anomalous westward currents the role of pushing back the warm pool to the west through zonal advection. The first three vertical modes contribute to these downwelling Rossby wave, but due to differences in wave speed, the first baroclinic mode Rossby wave extends farther west than the second and third baroclinic mode contribution, acting more constructively to the reversal toward cooler conditions at the mature stage of the cooling.

In November 1997, the Rossby wave amplitude along the equator at 120°W is 1.5 cm (-7 cm s^{-1}), 4.0 cm (-10 cm s^{-1}) and 2.5 cm (-5 cm s^{-1}), respectively, for the first, second and third baroclinic mode contribution to SLAs (ZCAs). At that time, large westerly wind anomalies force strong downwelling Kelvin waves with a larger amplitude for the second baroclinic mode than for the first baroclinic one, because the wind variability has moved eastward. Starting in July 1997, the Kelvin wave's amplitude for the second baroclinic mode increases along the wave path and at each pulse, whereas it decreases for the first baroclinic mode (see Fig. 6). In December 1997, the second baroclinic mode contribution to sea level and zonal current anomalies is dominant in the eastern Pacific. The second baroclinic mode Kelvin wave associated with the November 1997 wind event induces large westward anomalous currents through the reflected Rossby wave at the eastern boundary. Note the coherency between the Rossby wave amplitude and the 28°C isotherms in Fig. 6 at that time.

These conditions will last until June 1998 in the eastern Pacific for the second baroclinic mode, giving time for the zonal SST gradient to build up and to zonal advection to act onto SST changes. Note that in the eastern Pacific, there is a relatively weak contribution of the first baroclinic mode upwelling Kelvin waves in early 1998, compared to the second baroclinic Rossby wave contribution, suggesting that the mechanism at work for terminating the 1997–1998 El Niño may not involve the delayed action oscillator which attributes to the upwelling Kelvin wave reflected at the western boundary the reversal to the cold conditions.

4. REFLECTIVITY ON THE MERIDIONAL BOUNDARIES

The two main difficulties when determining the reflectivity power of the meridional boundaries for the long equatorial waves in the tropical Pacific, are: 1 – Separating the contribution of the local wind forcing from the part resulting from the reflection of the Kelvin waves near the western boundary and to the Rossby waves near the eastern boundary. 2 – Interpreting the decrease in amplitude of the Rossby waves as it propagates westward especially near the eastern boundary. It can be due to dissipation induced by non-linear processes and vertical propagation of energy [13]. In this study but not in earlier work, the vertical propagation of energy is explicitly taken into account as the horizontal mode decomposition is performed for all the baroclinic modes.

In order to determine the contribution of local wind forcing to the waves, a multi-mode simulation was performed with the linear model parameter values for phase speed (c_n) and projection coefficient (P_n) derived from the vertical mode decomposition of the OGCM. The linear model was forced with the ERS+TAO wind stress anomalies as for the assimilated run with a 5 day time step. A zonally varying projection coefficient ($P_n(x)$) was used. Wave reflections were cancelled at the meridional boundaries in order to consider only the contribution of the local wind forcing to the wave contribution (i. e. there is no contribution of reflected waves). Kelvin and *n*-meridional mode Rossby coefficients for each baroclinic mode are then derived.

Reflection efficiency is estimated by calculating the ratio of the incoming free wave amplitude (locally wind-forced contribution is retrieved) over the outgoing wave amplitude near the meridional boundaries. This is equivalent to compute the following quantities:

Near the western boundary,

$$cw_{m,n}(x,t)=\frac{(ak_m-ak_m^{wind})(x,t-\delta t_m(x))}{rn_m(x=145°E,t)}$$

and near the eastern boundary,

$$ce_{m,n}(x,t)=\frac{(rn_m-rn_m^{wind})(x,t+\delta t_m(x))}{ak_m(x=90°W,t)}$$

$\delta t_m(x)$ is the time needed for the waves to travel from 145°E (90°E) to the longitude *x* as a m^{th} baroclinic mode Rossby (Kelvin) wave and then as a reflected m^{th}-baroclinic mode Kelvin (Rossby) wave. ak_m and rn_m are the coefficients derived from ASSIM (cf. section 3). For the first(third)-meridional mode (*n=1(3)*), linear theory predicts that for an infinite meridional wall: $cw_{m,n}$(x=145°E,t)=0.41 (0.13) and $ce_{m,n}$(x=90°W,t)=1.22 (0.94).

Fig. 7 displays the results for the first two baroclinic modes. Higher-order baroclinic modes are not considered because there are much less energetic and propagate very slowly so that the contributions of the reflected waves are small. Higher-order meridional modes are not considered either for the same reasons.

Figure 7: reflection efficiency factor for Kelvin and first-meridional Rossby waves at the (top) eastern and

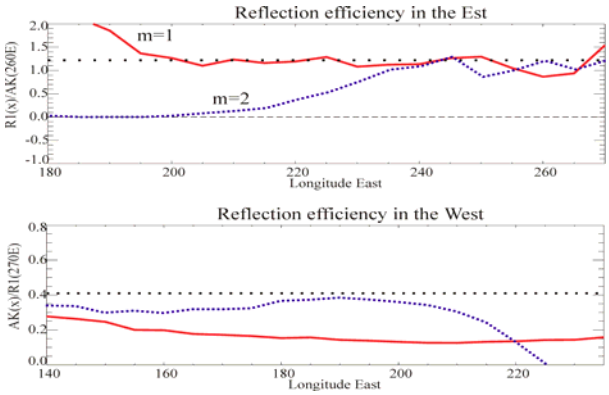

(bottom) western boundaries for the two gravest baroclinic modes (red=mode 1; blue=mode 2). The horizontal black dotted line gives the theoretical level (i.e. for an infinite meridional wall with no local wind forcing, dispersion or dissipation.).

As for the reflection at the eastern boundary, the results indicates that the American coast behave almost as an infinite meridional wall for the long equatorial waves reflection, since values are close to the theoretical value from 90°W to 130°W for both baroclinic modes, and as far as 160°W for the first baroclinic mode. The decrease of reflection efficiency west of 130°W may be due to an inaccurate estimation of the wind forcing contribution to the Rossby wave coefficient since we use an empirical formulation for dissipation in the linear model. However, we expect from the higher-order baroclinic mode waves that they do not extend to the west as much as the first baroclinic mode waves since they are associated to the vertically propagating variability (cf. [13]). Hence, from 130°W westward, one can consider that the eastern boundary is not "a reflector" of second baroclinic mode Kelvin waves.

At the western boundary (~140°E), the reflection efficiency is below the theoretical level by about 25% for both modes, suggesting a reflection

efficiency of 75% of that of an infinite meridional wall. It decreases slowly eastward leading to reflection efficiency of 45% at 170°W. For the second baroclinic mode, the reflection efficiency remains at an average level of 80% between 140°W and 150°W and then decreases sharply as the forced Kelvin waves are locally forced. Note that in the western Pacific, the second baroclinic mode contribution is much weaker than the first baroclinic mode contribution so that a fair estimate of the actual reflection efficiency of the western boundary is given (dominated) by the one of the first baroclinic mode , i.e. ~50% of an infinite meridional wall at ~165°E.

5. CONCLUSIONS

A forced Ocean General Circulation Model simulation of the tropical Pacific in which combined TOPEX/POSEIDON and ERS altimetric data over January 1994-July 1999 are assimilated, is used to investigate equatorial wave characteristics during the intense 1997-1998 El Niño-La Niña event. The assimilation results in an increased contribution of the higher-order baroclinic modes in the eastern basin and a decreased contribution of the first baroclinic mode in the western Pacific for the zonal current variability. Kelvin and first meridional Rossby waves are then derived for the first two more energetic baroclinic modes. The Kelvin waves of both modes contribute constructively to the strong warming observed in 1997, with the first (second) baroclinic mode being more energetic than the (first) second baroclinic mode in the early (mature) stage of the warming. Kelvin waves of both modes reflects as first meridional Rossby waves at the eastern boundary (reflection efficiency of ~ 95%) and contribute to push back the warm pool westward. From January 1998, the reversal of the warming is apparently initiated by the second baroclinic mode contribution which controls the position of the 28°C isotherm at the surface. At the western boundary, reflection of Rossby waves takes place for both modes, but a ~50% reflection efficiency is derived at 165°E. This suggests that the delayed oscillator theory is not applicable for explaining the reversal from warm to cold conditions during the 1997-1998 El Niño-La Niña, while the zonal advective feedback was at work. This study suggests that it is necessary to take into account the vertical structure of the ocean when interpreting altimetric data, which can be done through assimilation experiment.

6. REFERENCES

1. Dewitte, B., G. Reverdin and C.Maes, Vertical structure of an OGCM forced simulation of the tropical Pacific in 1985-1994. *J.Phys.Oceanogr*., 29, 1542-1570; 1999.
2. McPhaden, M., and X. Yu, Equatorial waves and the 1997-1998El Niño, Geophys. Res. Letter, 26, 2961-2964, 1999.
3. McPhaden, M., Genesis and evolution of the 1997-98 El-Niño. *Science*, 283, 950-954, 1999.
4. Parent, L., C. E. Testut, J. M. Brankart, J. Verron, P. Brasseur, and L. Gourdeau, Comparative assimilation of Topex/Poseidon and ERS altimeter data and of TAO temperature data in the tropical Paci¯c ocean during 1994-1998, and the mean sea-surface height issue, J. Mar. Syst., 40 41, 381-401, 2003.
5. Madec, G., P. Delecluse, M. Imbard, and C. Levy, OPA 8.1 Ocean General Circulation Model reference manual, *Nodes du pole de modélisation, Institut Pierre Simon Laplace (IPSL), France, 11*, 91pp, 1999.
6. Menkes C. and coauthors, Impact of TAO vs. ERS wind stresses onto simulations of the tropical Pacific Ocean during the 1993-1998 period by the OPA OGCM. *Climate Impact of Scale Interactions for the Tropical Ocean-Atmosphere System*, pp. 46-48, Euroclivar Workshop Report, Eucliv., 13, 46-48, 1998.
7. Reynolds, R. W., and T. M. Smith, Improved global sea surface temperature analyses using optimum interpolation. *J. Climate*, **7**, 929-948, 1994.
8. Pham D. T., J. Verron and M. C. Roubaud, A singular evolutive extended Kalman filter for data assimilation in oceanography, *J. of Marine Systems*, 16, 3-4, 323-340, 1998.
9. Verron, J., L. Gourdeau, D. T. Pham, R. Murtugudde and A. J. Busalacchi, An extended Kalman filter to assimilate satellite altimeter data into a non-linear numerical model of the tropical Pacific Ocean: Method and validation. *J. Geophys. Research*, 104, 5441-5458, 1999.
10. Cane, M. A., A. Kaplan, R. N. Miller, B. Tang, E. C. Hackert and A. J. Busalacchi, Mapping tropical Pacific sea level: Data assimilation via a reduced state Kalman filter, *J. Geophys. Res*, 101, *C10*, 22,599-22,617, 1996.
11. Gourdeau, L., J. Verron, T. Delcroix, R. Murtugudde and A.J. Busalacchi, Assimilation of Topex/Poseidon altimetric data in a primitive equation model of the tropical Pacific Ocean during the 1992-1996 ENSO period. *J. Geophys. Res.*, 105 C4, 8473-8488, 2000.
12. Picaut, J., F. Masia, and Y. DuPenhoat, An advective-reflective conceptual model for the oscillatory nature of ENSO, *Science*, 277, 663–666, 1997.
13. Dewitte, B. and G. Reverdin, Vertically propagating annual and interannual variability in an OGCM simulation of the tropical Pacific ocean in 1985-1994. *J. Phys. Oceanogr*., 30, 1562-1581, 2000.